"Structural and Mechanical Characteristics of Al -Pb Alloys produced by chill-Block melt spinning"

Mustafa Kamal, Abu-Bakr El-Bediwi, and Samira El-Mohamady Fouda*
Metal physics lab-physics Department
Faculty of Science Mansoura University Egypt
Email: kamal42200274@yahoo.com
Email: eng_mohamed201220125@yahoo.com
*M.Sc Student in Experimental physics (Metal physics)

***Abstract*-- Al-Pb monoetectic alloys with different compositions were rapidly solidified from melt using chill-block melt –spin technique. The rapidly solidified ribbons were investigated by X-ray diffraction (XRD) technique. The results showed that the structures of all melt-spun ribbons were completely composed two distinct phases of aluminium rich phase and lead rich phase. Additionally, Elastic moduli, Internal friction , thermal diffusivity and hardness measurements of melt-spun ribbons were examined by using Dynamic resonance method and Vickers indentor for one applied load of 10 grams of force for 5 seconds .The results also show that this material is very sensitive to the compositions.**

***Index Term* - Elastic Moduli – Internal friction , Thermal diffusivity , hardness measurements , monotectic alloys , XRD , Dynamic resonance method , melt-spin technique – Shear Stress .**

I. INTRODUTION

Monotectic alloys have attracted the interests of many scientists, since they are synthesized to perform specific functionality. In recent years the solidification studies of immiscible alloy systems is important from scientific and technical point of view (1, 2). Al-Pb alloys are a traditional alloy system which some with a miscibility gap in the liquid state (3). These kinds of alloy system have commonly accepted for having excellent mechanical and tribological for engineering applications. Since the early 1990 s, there has been significant research devoted to the melting and crystallization of Pb precipitates embedded in Al matrices (4, 5). Much of the work on Al-Pb as a simple monotectic phase diagram (figure 1) with negligible mutual solubility in the solid –solid and solid –liquid domains have been aimed at a better understanding of nucleation phenomena associated with melting and freezing of small confined particles.

The key physical parameters for nucleation of a second liquid phase in Al-Pb monotectic liquids had been measured by Kaban et al (6). Recently by Ning yang et al (7), significant progress had been achieved in computational materials science, and, as a powerful tool, molecular dynamics simulation was used to observe and control the cluster structures and the properties of the Al-Pb alloys. Although Al-Pb monotectic alloys have been under investigation since a few decades , the essential processes forming the mechanical properties of these alloys while passing the miscibility gap are not understood .The aim of this investigation was to develop cheaper substitutes for the common but expensive low melting bearing alloys include , alloys of the lead –base babbits (8) and aluminium base bearing alloys (9) using chill-block melt spinning technique (10) .

II. EXPERIMENTAL PROCEDURE

The experiment techniques utilized have been described in details (8, 11, and 14) and will be explained here in briefly. The melt –spun ribbons of Al-Pb monotectic alloys were prepared by melt-spinning with the compositions presented in Table I

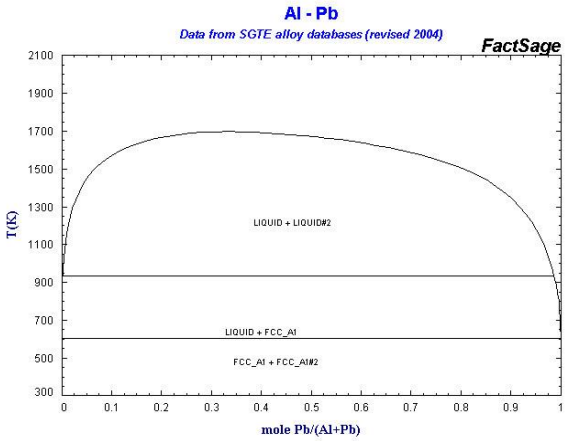

Fig. 1. A Simple phase diagram of Al-Pb monotectic Alloy

Table I

Al-0.9 wt % Pb
Al-1.2 wt % Pb
Al-5 wt % Pb
Al-10 wt % Pb
Al-20 wt% Pb
Al-30 wt % Pb
Al-50 wt % Pb

The Solidification front velocity in the ribbon was estimated to be 30.4 $m.s^{-1}$. Due to the small thickness of the melt-spun ribbons, the cooling rates can be assumed to be very high. The melt-spun ribbons are analyzed by X- ray diffraction technique of Al-0.9 wt %Pb , Al-1.2 wt % Pb , Al-5 wt % Pb , Al-10 wt % Pb , Al-20 wt % Pb , Al-30 wt % Pb , Al-50 wt % Pb with Cu Kα radiation . The resulting X-ray diffractograms are presented in figure (2). Techniques used for the subsequent characterization were dynamic resonance and vicker micro-hardness tester using loads of 10 grams of force for 5 seconds .

(a)

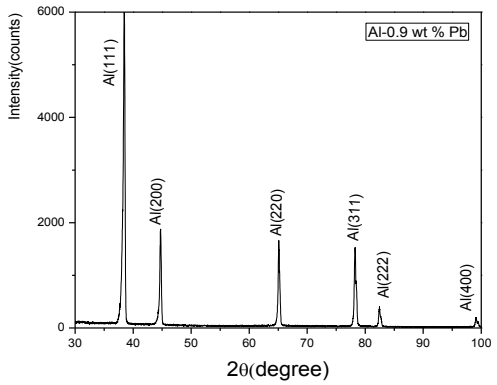

(b)

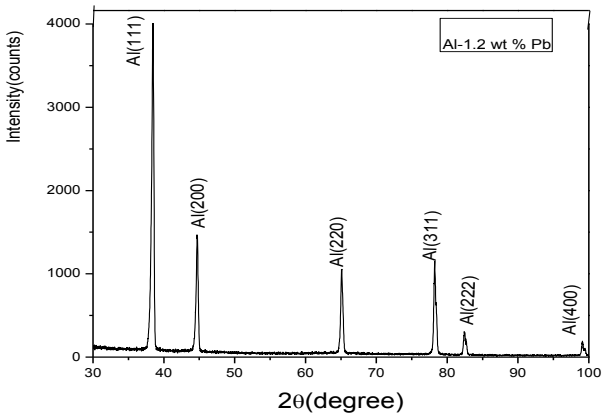

(c)

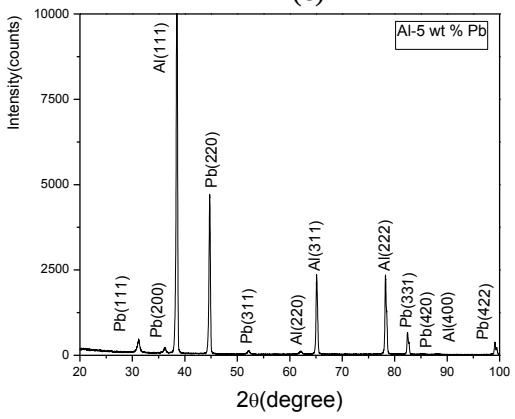

(d)

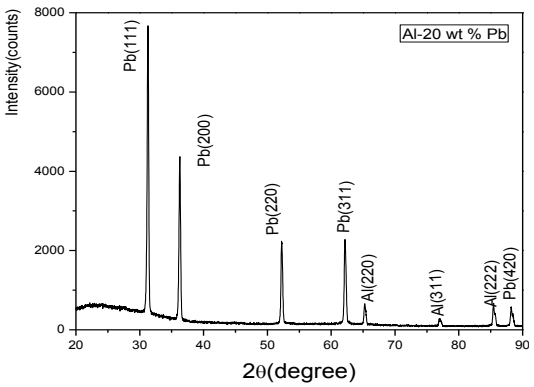

(e)

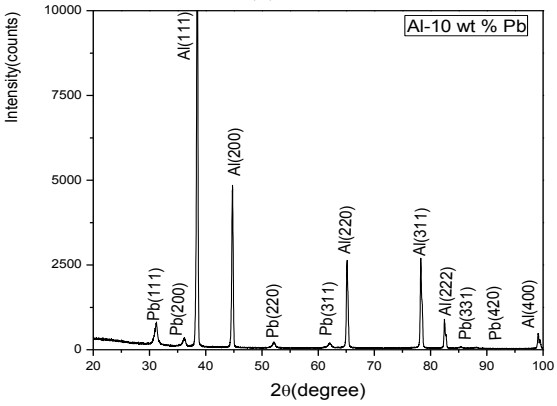

(f)

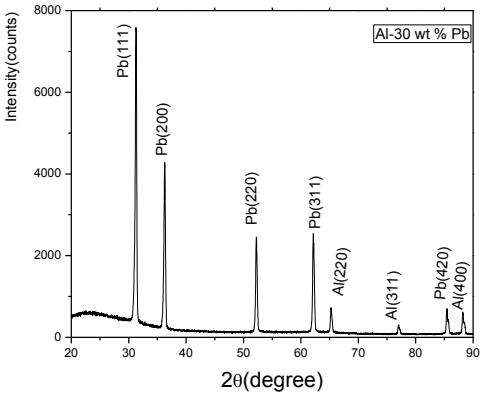

(g)

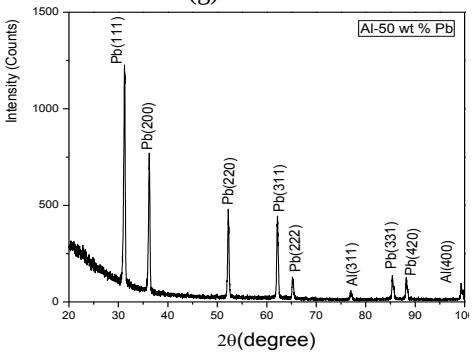

F ig. 2. Comparative x-ray diffraction scans for Al-Pb rapidly solidified from melt fig. 2 (a , b , c , d , e ,f , g)

III. RESULT AND DISCUSSIONS

Structural Information by X- ray Diffraction.

The experimental Al-Pb phase diagram as indicated in figure (1) .The phase diagram showed that no solid solubility, Suggesting very weak Al-Pb bonds vs. Al-Al and Pb-Pb

Table II

Element	Atomic radius (A^o)	Electronegativity (Pauling Scale)	Common valences'	Crystal structure	Density ($g . cm^{-3}$)
Al	1.43	1.61	+3	F.C.C	2.70
Pb	1.75	1.87	+2 , +4	F.C.C	11.34

In this system (15) part of the scientific problem in our study is that lead and aluminium have little in common very different atomic radii and electronegativity and no common valences as indicated in Table II, in addition they have very different densities.

Monotectic alloys undergo an invariant reaction at the monoetectic temperature, in which a liquid phase, L1, is decomposed into a solid phase, S, and a liquid phase L2. The X- ray diffractograms in figure (2) reveals the preliminary phase identification in the melt-spun ribbons. All the recorded diffraction peaks at the same value of 2Θ , denoting the presence of lead and aluminium only with F.C.C structure .The pattern shows the existence of two kinds of phase with face centered cubic structure . X- ray diffraction is a tool for the investigation of the fine structure of metals and metal alloys and to study of phase equilibria of the ensemble of orientations in a Polycrystalline aggregate. A cubic crystal gives diffraction lines whose $\sin^2\theta$ value, satisfy the following equation , obtained by combining the Bragg law with the plane-spacing equation for the cubic system :

$$\frac{\sin^2\theta}{\left(h^2+k^2+l^2\right)} = \frac{\lambda^2}{4a^2} \qquad [1]$$

Since the sum ($h^2+k^2+l^2$) is always integral and $\lambda^2/4a^2$ is a constant for any one pattern , the problem of indexing the pattern of a cubic substance is one of finding a set of integers ($h^2+k^2+l^2$) bonds This also explains why no intermediate solid phase form which will yield a constant quotient when divided one by one into then observed $\sin^2\theta$ values (16) . The crystal structure of the melt-spun Al-Pb alloys, it was suggested to be a cubic cell based on X- ray diffraction investigations (17). X- ray diffraction charts in which Cu Kα radiation was used is shown in figure (2) .The new peaks representing the metastable phase are evident. Because the melt-spun ribbons of Al-0.9 wt %Pb , Al-1.2 wt % Pb , Al-5 wt % Pb , Al-10 wt % Pb , Al-20 wt % Pb , Al-30 wt % Pb , Al-50 wt % Pb were composed of a mixture of both the metastable phase and the stable elements(Al , Pb) for the equilibrium phase are also present . Because there were three phases in the present melt-spun ribbons (aluminium, lead, and metastable phase) , Some peaks were very close to each other on even overlapped . The crystallographic nature of different phases in the melt-spun alloys particles were determined by systematic fitting of the sample to different prominent zone axes of the matrix. Analysis of these diffraction patterns indicates that the two phases are equilibrium Al and Pb having cubic structure. Lead in such particles exhibits an orientation relationship with the aluminium matrix. Results for lattice parameter are listed in Table III.

Table III

Element	Lattice parameter (A^o)
Al-0.9 wt % Pb	4.0490
Al-1.2 wt % Pb	4.0513
Al-5 wt % Pb	4.0501
Al-10 wt % Pb	4.0509
Al-20 wt% Pb	4.077
Al-30 wt % Pb	4.1076
Al-50 wt % Pb	4.1095

The lattice parameters of aluminium phase increased steadily with increasing alloying content as shown in figure (3) reaching a value of (4.1095 A^o) for the Al-50wt%Pb ribbons . The increase in the lattice parameter of aluminium phase with lead indicates that the amount of dissolved lead has increased. So it is , an important results in our case indicating that the melt-spinning technique enhanced the solubility limit of lead in aluminium as a good material used in bearing applications (17 , 2)

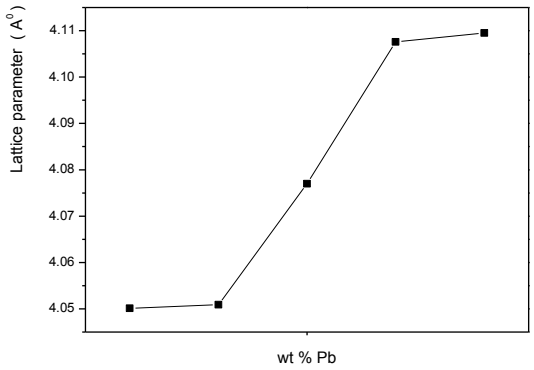

Fig. 3. Lattice parameters versus Pb concentration for liquid-quenched Al rich FCC phase

Determination of the number of atoms in a unit cell

The next step after identifying the phases of the unit cell is to find the number of atom in the unit cell. To find this number we use the fact that the volume of the unit cell , calculated from the lattice parameters multiplied by the measured density of the melt-spun ribbons equals the weight of the all the atoms in the cell , for any crystal:

Density=Weight of atoms in unit cell / Volume of unit cell

Or

$$\rho = \frac{\varepsilon A}{N V} \qquad [2]$$

if V in Equation [2] for the density of a crystal is expressed in A^3 and the currently accepted value of Avogadro 's number N inserted , then the equation [2] becomes

$$\varepsilon A = \rho V/1.66020 \qquad [3]$$

$$\varepsilon A = n A \qquad [4]$$

Where n is the number of atoms per unit cell and A is the atomic weight. Results for the number of atoms per unit cell of as spun Al-Pb ribbons are listed in table [IV] .

Table IV

System	Number of atoms / unit cell	Volume of the unit cell (A^3)	Density ($gm.cm^{-3}$)
Al as a bulk	4	66.4	2.7
Al as spun ribbon	3.7	66.49	2.494
Al-0.9 wt % Pb	3	66.45	2.05
Al-1.2 wt % Pb	3.6	66.38	2.44
Al-5 wt % Pb	2.22	66.45	1.99
Al-10 wt % Pb	1.88	66.46	2.11
Al-20 wt% Pb	6	65.41	9.49
Al-30 wt % Pb	4.66	73.50	8.53
Al-50 wt % Pb	3.5	67.72	9.79

The number of atoms per unit cell in any crystal is partially dependent on its Bravais lattice. So when determined in this way , the number of atoms per cell is always an integer such as in the bulk sample of aluminium pure , within experimental

error , except for some which have defect structures . In our case melt-spun ribbons , atoms are simply missing from a certain fraction of these lattice sites which they would be expected to occupy , and the result as shown in Table {IV} is a non integral number of atoms per cell .

Lattice disorder in Al-Pb rapidly quenched from melt

Melt –spun ribbons of monotectic Al-Pb immiscible alloys has been shown to produce appreciable changes in the intensity substances distribution of diffracted X-rays. The most prominent of these effects are changes in integrated intensity and changes in line shape (18, 19). Line width B , both the full width at high maximum intensity of the peak , FWHM and integral , were used in a Williamson Hall plot (19) as illustrated in figure (4) , to derive information about the size of coherent zones (crystallite size D_{eff}) and the local lattice distortions $< \varepsilon^2 >$ in all phases (20) .

$$B = \frac{1}{D_{eff}} + 5 < \varepsilon^2 >^{1/2} \mathrm{Sin}\frac{\theta}{\lambda} \qquad [5]$$

The $1/D_{eff}$ and $5 < \varepsilon^2 >^{\frac{1}{2}}$ parameters are given in Table V

Table V

System	Particle size (A^o)	$1/D_{eff}$ (A^{o-1}) *10^{-3}		$5 < \varepsilon^2 >^{1/2}$ (10^{-4})	
		Al	Pb	Al	Pb
Al-0.9 wt % Pb	497.7	2.1		8.6	
Al-1.2 wt % Pb	467.2	2.2		9.2	
Al-5 wt % Pb	277.8	4.6	4.1	12.3	23.6
Al-10 wt % Pb	247.8	4.1	5.7	13.8	23.6
Al-20 wt% Pb	521.9	2.4	2.1	9.1	9
Al-30 wt % Pb	462.3	2	2.3	7.7	9.6
Al-50 wt % Pb	454	2.3	3.2	9.3	13.4

For the aluminium phase, as well as for Pb phase, $1/D_{eff}$ is unmeasurably low, hinting to a good crystallization state as indicated in figure (4).

(a)

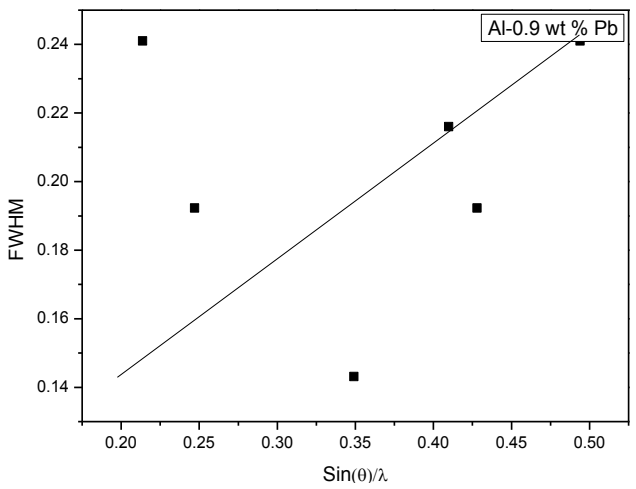

(b)

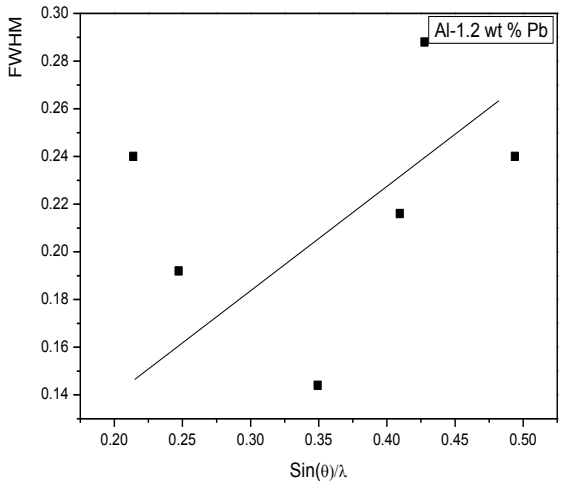

(c)

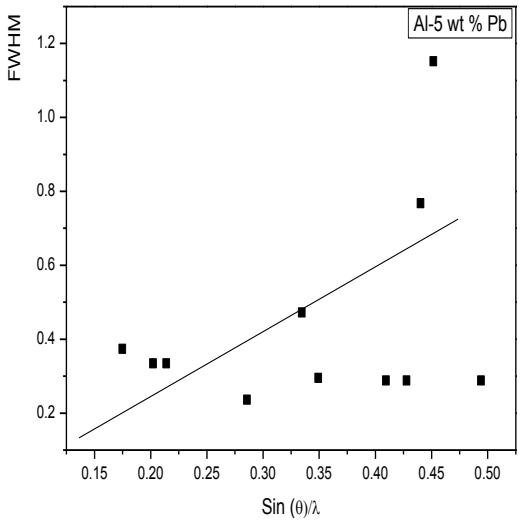

(f)

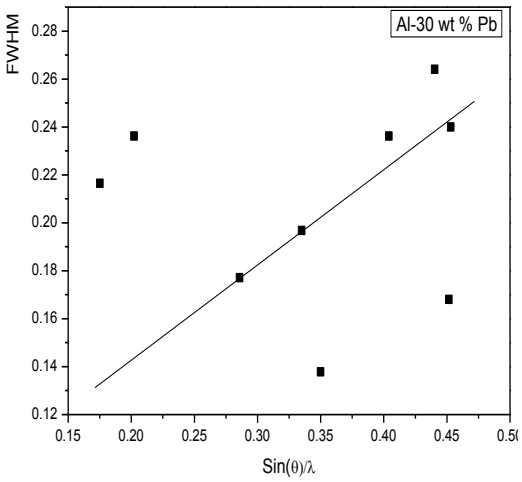

(d)

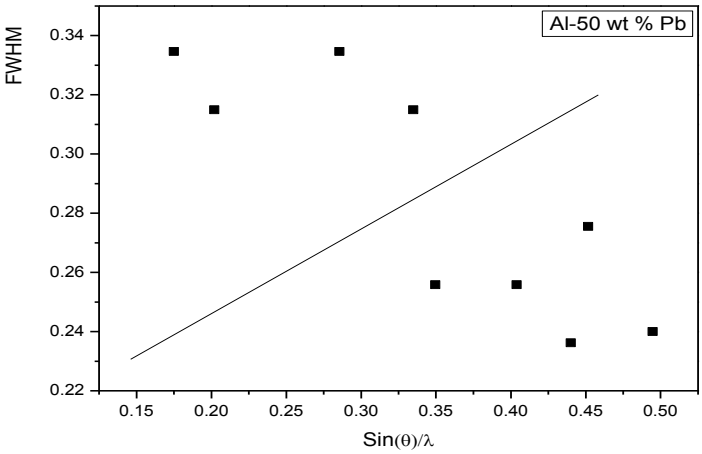

(g)

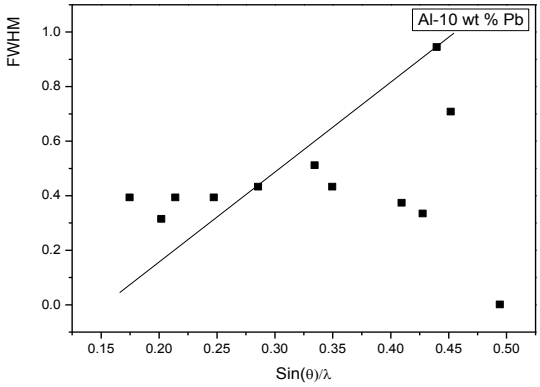

Fig. 4. (a , b , c , d , e , f , g)

(e)

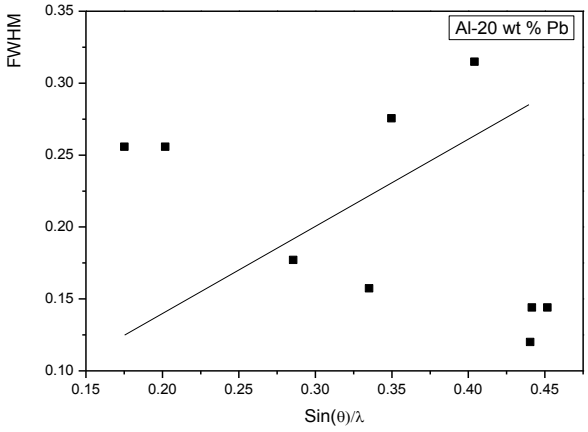

Lattice distortions for both Al and Pb phases are lower for Al-5 wt % Pb and Al-10 wt % Pb as spun ribbons than for Al-20 w t% Pb, Al-30 wt % Pb, and Al-50 wt% Pb. This supports that phase Pb is more disordered than aluminium phase for both compositions supporting the stacking-fault segregation origin of the Pb lattice. In the cubic lattice the twelve immediate neighbors' are equivalent. It is quite obvious that as a result of some effect the otherwise regular stacking sequence becomes disordered, and stacking fault is created , for instance in the following way:

↓

. . . ABC ABABC ABC . . .

At the position denoted by the arrow there is a stacking fault. Since two layers of identical character cannot follow by introducing the stacking operator (21). Stacking faults are created whenever there is more than one possibility for the

arrangement of the atomic layers. The more complicated the structure , the more numerous are the possible stacking orders

Elastic moduli and Internal friction Q^{-1}

Table VI

System	E (G Pa)	G (G Pa)	K (G Pa)	$Q^{-1} *10^{-4}$	Poisson ′s ratio
Al-0.9 wt % Pb	54.7	20.3	61.1	555	0.35
Al-1.2 wt % Pb	45.6	16.9	51.1	546	0.35
Al-5 wt % Pb	37.2	13.7	42.8	370	0.355
Al-10 wt % Pb	27.2	9.99	32.1	387	0.359
Al-20 wt% Pb	11.7	4.28	14.8	1249	0.368
Al-30 wt % Pb	11.1	4.04	15.1	646	0.377
Al-50 wt % Pb	11.8	4.21	18.7	1251	0.395

works with polycrystalline materials such as in our case "melt -spun ribbons ", in which the individual crystallites are arranged completely randomly, it can generally be assumed that the mechanical properties of materials are isotropic. Then quite simply relationships exist between the elastic constants (22)

$E=3K (1-2 \nu)$ [6]

And

$E=2G (1+\nu)$ [7]

Where E is the Young ′s modulus, G, the shear modulus, K is the bulk modulus and ν is the poisson ′s ratio. The trend in developing new bearing alloys can be viewed as the opportunity to improve device performance and reliability. The interesting trend in this field is that high mechanical strength combined with good ductility tends to increase fatigue life (23, 24). Measured values are listed in Table {VI} , For The constant of proportionality between stress and strain is called a modulus of elasticity. Young′s modulus E , shear modulus G , bulk modulus K and internal friction Q^{-1}evolutions as a function of lead content for samples Al-0.9 wt %Pb , Al-1.2 wt % Pb , Al-5 wt % Pb , Al-10 wt % Pb , Al-20 wt % Pb , Al-30 wt % Pb , Al-50 wt % Pb rapidly solidified from melt using melt-spinning technique . These measurements were performed with the vibrating reed apparatus in the ranging from 10 Hz to 100 Hz frequency range. The data indicate that the shear stiffnesses of the various melt-spun ribbons of Al-Pb monotectic alloys are sensitive to composition. For the melt-spun Al ribbons , the elastic modulus from about Al-0.9 wt % Pb and up to Al-5 wt % Pb additions it is ranging from 52 G Pa to 37 G Pa and then suddenly decreased , whereas coarse-grained lead shows substantially a decreasing trend by increasing the lead addition up to Al-50 wt % Pb.

These elastic moduli are usually anisotropic in the case of single crystals, but, since the mechanical engineer usually

As regards the Q^{-1} behavior (Table (VI), in all melt-spun ribbons the background damping rises with lead additions. The problem of understanding the intrinsic anelastic behavior of melt-spun ribbons of Al -Pb immiscible alloys by dynamic resonance method is not unequivocal clear cut . There are some reasons for that: the melt spun ribbons prepared by melt-spinning technique, the results are affected by extrinsic structural parameters, such as the porosity, the melting temperature and the densification behavior of Al-Pb alloys. A low level of Q^{-1} for Al-5 wt % Pb and Al-10 wt % Pb rapidly solidified from melt implies a rigid structure which may be due to the absence or the locking of crystal defects (25) .

Thermal diffusivity

The linear law relating heat flow and temperature gradient gives only a partial description of the thermal processes involved in solids. This can be expressed in terms of the Fourier ′s law

$$U= -ג \text{ grad } T \qquad [8]$$

Where U is heat current, ג thermal conductivity, T absolute temperature and the minus sign arises from the fact that heat

always flows from the hotter to the colder region. The changes in internal energy can be expressed in terms of the specific heat C multiplied by the density ρ

$$C\rho\frac{dT}{dt} = -div\ U = div(\lambda\ grad\ T) \quad [9]$$

Where t is time the form of this equation allows for the possibility of the thermal conductivity varying with position , either owing to the temperature gradient or to actual in homogeneity of the result-spun ribbons used . So the equation [9] is written

$$\frac{dT}{dt} = D_{th}\ \nabla^2 T \quad [10]$$

Where $D_{th} = \frac{\lambda}{c\ \rho}$ is called thermal diffusivity. Equation [10] is essential in the discussion of time-varying thermal phenomena in homogeneous media ; there are appropriate modification to allow for anisotropic conductors (26) .The value of thermal diffusivity D_{th} , of (Al-0.9 wt %Pb , Al-1.2 wt % Pb , Al-5 wt % Pb , Al-10 wt % Pb , Al-20 wt % Pb , Al-30 wt % Pb , Al-50 wt % Pb) melt-spun ribbons controls the time rate at which the melt-spun ribbons with a non uniform temperature reaches a state of thermal equilibrium. The mathematical formula that relates thermal diffusivity D_{th} to the resonance frequency f_o at which the peak damping occurs using the dynamic resonance method (27) is

$$D_{th} = \frac{2\ d^2\ f_0}{\pi} \quad [11]$$

where d is the thickness of the melt-spun ribbon . The specific heat ,C of the melt-spun ribbons can be expressed in terms of the resonance frequency f_o and the thickness of the ribbons d ; by introducing equation of thermal diffusivity in equation [12] we have

$$\frac{2\ d^2\ f_0}{\pi} = \frac{\lambda}{c\ \rho} \quad [12]$$

The thermal conductivity of the melt-spun ribbons of the samples used in this study can be expressed in terms of the electrical conductivity using the modified Wiedeman-Franz ratio (28 , 29) ; ג (thermal conductivity)

$$= 5.02\sigma\ T\ x10^{-9}+0.03 \quad [13]$$

Where σ is the electrical conductivity and T is absolute temperature. The thermal diffusivity, and the electrical conductivity of melt-spun ribbons of (Al-0.9 wt %Pb , Al-1.2 wt % Pb , Al-5 wt % Pb , Al-10 wt % Pb , Al-20 wt % Pb , Al-30 wt % Pb , Al-50 wt % Pb) as a function of lead content are depicted in table {VII} .

A non linear increase of thermal diffusivities with an increase in lead content is observed in all case. It is assumed that this fact is caused by some aggregation of lead particles , particularly the distribution of lead particles is important in determining the effective spreading of lead in forming a layer of solid lubricating , while employed in a bearing .

Microhardness measurements

The mechanical properties of melt-spun ribbons of Al-Pb monotectic alloys were determined by Vickers micohardness measurements. As performed on preceding literature studies (30, 31). The values were calculated using the standard Vickers formula ,

$$Hv = \frac{2\ Sin68\ (P)}{d^2} = \frac{1.8544\ (P)}{d^2} \quad [14]$$

Table VII

System	Thermal Diffusivity (10^{-10} $m^2.sec^{-1}$)	Specific heat (10^2J/kg.°C)	Thermal Conductivity ($10^{-2}W\cdot m^{-1}\cdot K^{-1}$)	Electrical conductivity ($10^4\Omega^{-1}.m^{-1}$)
Al-0.9 wt % Pb	940	30.3	58.3	37.5
Al-1.2 wt % Pb	13	2491.5	79	50
Al-5 wt % Pb	36	638.4	45.8	29.2
Al-10 wt % Pb	22	787.3	36.6	22
Al-20 wt% Pb	117	42.3	47	29
Al-30 wt % Pb	207	12.3	21.7	12.3
Al-50 wt % Pb	199	52.7	102.7	68

Where, P is the indentation force, d the average diagonal length and 1.8544 is a constant of a geometrical factor for the diamond pyramid. The calculated values for melt-spun ribbons (Al-0.9 wt %Pb , Al-1.2 wt % Pb , Al-5 wt % Pb , Al-10 wt % Pb , Al-20 wt % Pb , Al-30 wt % Pb , Al-50 wt % Pb) are given in Table by examining the table VIII

Table VIII

System	H_V (Pa)
99.1%Al_0.9%Pb	466.3
98.8%Al_1.2%Pb	312.9
95%Al_5%Pb	344.7
90%Al_10%Pb	468.7
80%Al_20%Pb	57.1
70%Al_30%Pb	39
50%Al_50%Pb	55

One can clearly see that the hardness value have the same value of pure aluminium as melt – spun ribbons and increased for Al-10 wt % Pb , then the microhardness values decreased . This increase can be interpreted as indication that the hardness of Al-Pb monotectic melt-spun ribbons is a function of the distribution of lead particles. It reveals that increase in lead content will result in lowering of the values of hardness. This can be attributed to the formation of lubricating film (32). The rise in hardness values can be due the effect of lead is greatly reduced. Hardness measurements however are more influenced by precipitate size of the distribution of lead particles which explain the behavior of the grain and cell sizes of the distribution of lead particles in the ribbons produced by melt-spinning technique.

Impact yield Stress and indention hardness

Hardness measurements can be used to obtain yield stresses for melt-spun ribbons used in this study and to estimate impact yield stresses (33). The maximum shear stress that is created by a locally applied pressure occurs on the central axis below the pressurized region as indicated by Timoshenko and Goodier (34). The maximum shear stress will be

$$\tau_m = 0.5H \{\tfrac{1}{2}(1-2\nu)+0.22(1+\nu)[2(1+\nu)]^{1/2}\} \quad [15]$$

Where ν is poissonṡ Ratio. The values of τ_m for Al-0.9 wt % Pb , Al-1.2 wt % Pb , Al-5 wt % Pb , Al- 10 wt % Pb , Al-20 wt % Pb , Al-30 wt % Pb , Al-50 wt % Pb as melt-spun ribbons are listed in Table {IX}

Table IX

maximum shear stresses for Al-Pb melt-spun ribbons

System	Maximum shear stress (Pa)	Friction (10^{-2}) (τ_m/ H)
Al-0.9 wt %Pb	162.6	34.87
Al-1.2 wt % Pb	109	34.86
Al-5 wt % Pb	120	34.81
Al-10 wt % Pb	163	34.76
Al-20 wt % Pb	19.7	34.64
Al-30 wt % Pb	13.5	34.52
Al-50 wt % Pb	19	34.28

From the Table {IX} it is showing that many familiar bearing materials contain two or more phases, with one phase ductile and another phase considerably harder. It is suggest that they work well. This would be consistent with familiar friction models (35) which indicate that friction (36) can be roughly estimated by the ratio of a shear stress to a hardness or yield pressure

Future work

According to our Experimental data, we introduce some criteria; they are based on the composition and atomic size factors in aluminium monotectic alloys rapidly solidified from melt using chill-block melt-spin technique (10).

CONCLUSION

The study concludes that melt-spin technique is an effective technique for producing a uniform dispersion of Pb droplets in aluminium monotectic alloys. The particle size in the

Aluminium phase become slightly smaller as the alloy composition was increased in the Al-Pb monotectic alloys. It also concluded that measured values of the elastic moduli and internal friction affect by extrinsic parameters, such as the porosity, the melting temperature and the densification of Al-Pb monotectic alloys. It is found that the distribution of lead particles is important in determining the effective spreading of lead in forming a layer of solid lubricating, while employed in bearing. Generally , It is concluded that the liquid-liquid disintegration can be initiated by a series of acts of nucleation of the second liquid phase in Al-Pb monotectic liquids

REFERENCES

(1) J. Z. Zhao and L. Ratke , Scripta Materiala , 50 (2004) , 543-546

(2) H. R. Kotadia, J. B. Patel, Z. Fan, E. Doernberg, and R. Schmid-Fetzer , TMS (The Minerals , Metals & Materials Society) , (2009) pp : 81-88 G. Korekt and L. Ratke, Materials Science Forum, Vols. 215-216 (1996) pp : 81-88

(3) G.Korekt and L. Ratke , Materials Science Forum, Vols.215-216 (1996) PP: 81 – 88

(4) K. L. Moore, D. L. Zhang, and B. Cantor, Acta Metall-mater. , (1990) , 38 , 1327

(5) A. Landa, P. Wynblatt, D. J. Siegel, J. B. Adams, O. N. Mryasov, and X. Y. liu , Acta mater . 48 (2000) 1753-1761

(6) I. Kaban, M. Kohler, L. Ratke, W. Hoyer, N. Mattern, J. Eckert, and A . L. Greer , Acta Materialia , Volume 59 , Issue 18 , October (2011) pages 6880-6889

(7) Ning Yang , Yong Sun and Hui Zhang , Advanced of Materials Research Vols , 634-638 (2013) pp : 1840-1843

(8) Mustafa kamal, A. El-Bediwi, A. R. Lashin , A.H.EL-Zarka , materials science and Engineering A 530(2011)327-332

(9) M. Kamal, A.M.Shaban, M.El-Kady and R. Shalaby, second International conference on Engineering Mathematics and physics (ICEMP-94) Vol. 2 , pp .107-121(1994)

(10) Mustafa Kamal and Usama S.Mohammed, A. Review: Chill-Block Melt Spin Technique, Theories & Applications, (2012) ISBN: 978-1-60805-151-9, Bentham e Books, Bentham science publishers.

(11) M. Kamal, J. C Pieri , and R. Jouty , Memoires et Etudes Scientifiques Revue de Metallurgie Mars (1983) 143-148

(12) Mustafa Kamal, Abu-Bakr El-Bediwi, and Mohammed S. Jomaan , International Journal of Engineering & Technology , I J E T – I J E N S , No : 06 , (2012) 60-67

(13) Mustafa Kamal and El-said Gouda, Radiation Effects and Defects in Solids, Vol. 163, No. 3 Marsh (2008) 237-240

(14) Mustafa Kamal and Tarek El-Ashram, J. Mater. Sci : Mater Electron (2008) 19 : 91-96

(15) IMPRESS Education: Solidification, Intermetallics & Immiscible: 2013/02/22 "Not all mixtures of metals produce solid solutions. Two extreme cases are immiscible metals and Intermetallics"

(16) B. D. Cullity, Elements of x-ray diffraction, Addison-Wisley Series in Metallurgy and Materials, U. S. A: (1959) Ch. 10 , pp : 297-323

(17) Ch .V. S. H. S. R. Sastry, and G Ranga Janardhana, Indian Journal of Engineering & Materials Sciences, vol. 17 , February (2010) , pp : 56-60

(18) W. H. Hall, and G. K. Williamson, Proc. Phys. Soc. 64B (1951) 937 , 946

(19) G. K. Williamson, and W. H. Hall, Acta Metallurgica, Vol. 1, Jan. (1953) 22

(20) R. Manaila, F. Zavaliche, R. Popescu, D. Mcovei, A. Devenyi, C. Bunescu, E. Vasile, and A . Janu , Materials Science and Engineering A 226-238 (1997) 290-295

(21) I. Kovacs and L. Zsoldos , Dislocations and Plastic Deformations , Pergamen Press , (1973) page 165

(22) Mervyn Lovell , Alan Avery and Michael Vernon , Physical properties of Materials , English Language Book Society (ELBS) edition (1979) , 87-105

(23) W. B. Hampshire, in Electronic Materials Handbook, Vol. 1 : packaging (ASM International , Metals Park , Ohio , 1989) , P . 633

(24) M. Mc Comack, S. Jin, G. W. Kammlott, and H. S. Chen, Appl. Phys. Lett. 63 (1) , 5 July (1993) 15-17

(25) E. Bonetti, L. Del Bianco, L. Pasquini, and E. Sampaolesi, Nano structured Materials, Vol. 10, No. 5 , (1998) 741-753

(26) J. E. Parrot and Audrey D. Stukes , Thermal Conductivity of Solids , Pion limited , London N W 2 5JN (1975) Ch . 1

(27) Mustafa Kamal and El-Said Gouda, Radiation Effects & Defects in Solids, Vol. 162, No. 9 , September (2007) , 691-696

(28) Mustafa Kamal and Abu-Bakr El-Bediwi , Radiation Effects & Defects in Solids , November – December (2004) , Vol . 159. pp 651-657

(29) G. E. Doan, The principles of Physical Metallurgy, 3 rd. ed , McGraw Hill Book Company , New York (1953)

(30) M. Yan, W. Z. Zhou, B. Cantor, Mater. Sci. Eng. A 284 (2000) 77-85

(31) O. Uzun, T. Karaaslan, M. Goge bakan, M. Keskin , Journals of Alloys and Compounds 376 (2004) 149-157

(32) J. P. Pathak and S. Mohan, Bull. Mater. Sci, Vol. 26, No. 3. April 2003 , pp 315-30-Indian Academy of Sciences

(33) J. J. Gilman, Journal of Applied Physics, Vol. 46, No. 4 , April (1975) 1435

(34) S. Timoshenko and J. Coodier, Theory of Elasticity, 3 rd Ed. Mc Graw – Hill , New York , (1970) , P 407

(35) F. P. Bowden and D. Tabor , The Friction and Lubrication of Solids Oxford University press , Oxford , 1964

(36) J. Zhang, F. A. Moslehy and S. Rice , A model for friction in quasi-steady-state sliding , Part II : numerical results and discussion , Wear 149 (1991) 13-25